

RESONA: Improving Context Copying in Linear Recurrence Models with Retrieval

Xinyu Wang^{*†} Linrui Ma^{*} Jerry Huang^{*} Peng Lu
Prasanna Parthasarathi Xiao-Wen Chang Boxing Chen Yufei Cui

Abstract

Recent shifts in the space of large language model (LLM) research have shown an increasing focus on novel architectures to compete with prototypical Transformer-based models that have long dominated this space. Linear recurrent models have proven to be a viable competitor due to their computational efficiency. However, such models still demonstrate a sizable gap compared to Transformers in terms of in-context learning among other tasks that require recalling information from a context. In this work, we introduce RESONA, a simple and scalable framework for augmenting linear recurrent models with retrieval. RESONA augments models with the ability to integrate retrieved information from the provided input context, enabling tailored behavior to diverse task requirements. Experiments on a variety of linear recurrent models demonstrate that RESONA-augmented models observe significant performance gains on a variety of synthetic as well as real-world natural language tasks, highlighting its ability to act as a general purpose method to improve the in-context learning and language modeling abilities of linear recurrent LLMs.

1 Introduction

Improvements in building state-of-the-art LLMs (OpenAI, 2024; Grattafiori et al., 2024; Qwen, 2024; Gemma Team, 2024) through increased scale (Chung et al., 2024; Kaplan et al., 2020) and downstream tuning (Ouyang et al., 2022; Dubois et al., 2023) have enabled them to attain human-level performance on a number of complex tasks. One particular feature that has enabled such a feat is the use of in-context learning (Brown et al., 2020), where models can use user-provided content to provide a specific response tailored to that example. This relies on the Transformer (Vaswani et al., 2017) backbone that underlies many of these models, enabling for models to observe the complete past when generating content.

However, a growing trend is the emergence of linear recurrent models (LRMs) (Gu et al., 2022; Peng et al., 2023; Orvieto et al., 2023; Gu and Dao, 2024), aimed to address a number of computational bottlenecks related to the use of attention (Bahdanau et al., 2015). Unlike Transformer-based models, LRMs do not operate over all previous parts of the input but instead compress it within a unified hidden representation/state much like original recurrent neural networks (RNNs) (Rumelhart, 1989; Hochreiter and Schmidhuber, 1997; Cho et al., 2014), enabling for more efficient inference. However, this unified representation has been shown to also act as an information bottleneck, where the number of potential elements in the vocabulary cannot be properly maintained within a state that does not grow with the possible combinations of tokens. This has raised questions regarding the ability of such models to adequately learn from input contexts (Jelassi et al., 2024; Park et al., 2024; Grazzi et al., 2024) and perform comparably with similar Transformer-based LLMs in such settings.

Linear methods rely on fixed-size states to account limitations of traditional attention. A trade-off, however, is these fixed-size states cannot perfectly preserve all historical information, making exact retrieval challenging. This manifests itself in practice in various tasks such as language modeling; with the key-value associative memory system that underlies

[†]Corresponding author: Xinyu Wang (xinyu.wang5@mail.mcgill.ca), affiliated with McGill University, and Noah’s Ark Lab, Canada.

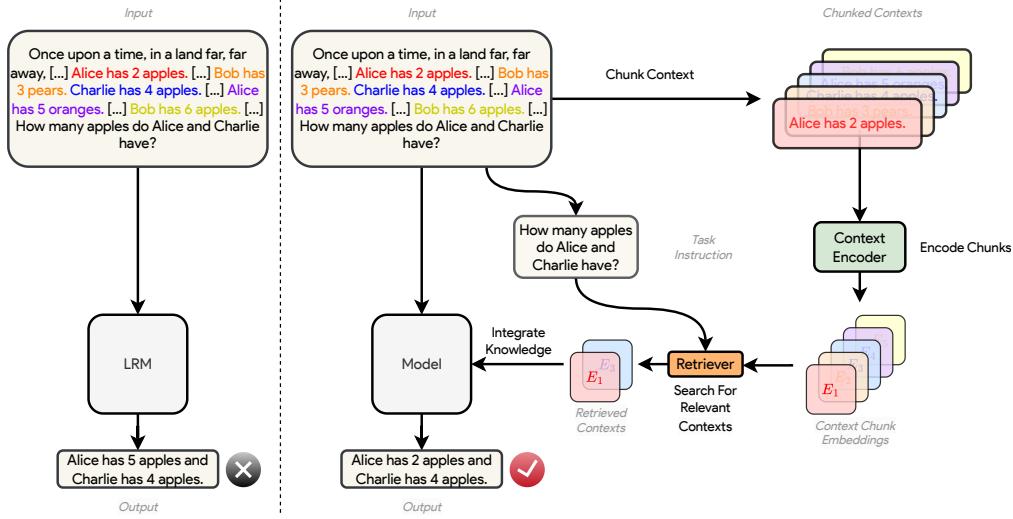


Figure 1: Simplified overview of RESONA. The input is separated into the example-specific context along with a task-specific instruction. The context is chunked and encoded, after which a retriever uses the instruction to determine which chunks are relevant to solving the task. The retrieved context is integrated into the model’s reasoning for improved response.

such methods, adding new key-value associations leads to accumulating retrieval errors that hinder performance. These errors can accumulate, whether it be data-independent (Gu et al., 2022; Orvieto et al., 2023) or dependent (Yang et al., 2024a; Gu and Dao, 2024; Peng et al., 2024; Zhang et al., 2024; Beck et al., 2017), and despite proposals to correct such errors (Yang et al., 2024b; 2025; Sun et al., 2024), these retain a fixed-size hidden state that cannot address the aforementioned limitation.

In an effort to bridge this gap, we introduce RESONA as a method to improve context-based learning in LRMs through retrieval, RESONA (Figure 1). we introduce a retrieval mechanism that enables the information flow from the context to overcome bottlenecks in the hidden state, enabling the model to better use it for in-context learning. First, specific LRM layers within the backbone model are augmented with RESONA, which consists of a mechanism that performs a contextual search on the input context, which we implement by chunking the context into passages and retrieving them based on the LRM state. This is followed by a knowledge-integration component that mixes the retrieved context back into the LRM output by directly modifying the output representation. This enables for information from the context to overcome the hidden state bottleneck, allowing for improved information flow from the context to the generated input. These processes (chunking, retrieval, and integration) are further parallelized with the main LRM, ensuring easy adaptation and improved in-context learning across a variety of models.

Empirical results on a set of representative tasks, both synthetic and real-world, demonstrate that RESONA significantly improves the abilities of LRMs to utilize context-specific information with minimal to no latency cost. We evaluate RESONA on a diverse set of tasks, including synthetic retrieval and recall tasks, language modeling and question-answering tasks, across multiple scenarios such as pre-training and direct-finetuning. Our analysis demonstrates the effectiveness of using RESONA for overall performance improvements as well as test-time model customizations, such as balancing the trade-off between efficiency and performance.

2 Related Works

Linear Recurrent Models. Despite the vast improvements in constructing language models that solve real-world natural language tasks since the introduction of the Trans-

former (Vaswani et al., 2017), significant concerns remain regarding the efficiency and scalability of such models. While this has spurred interest in rendering them more efficient (Katharopoulos et al., 2020; Dao et al., 2022; Yang et al., 2024a), LRMs (Gu et al., 2022; Orvieto et al., 2023; Qin et al., 2023; Gu and Dao, 2024; Dao and Gu, 2024; Peng et al., 2023) have grown as a popular alternative due to highly efficient inference costs compared to attention-based alternatives while retaining the ability to be trained on elements of a sequence in parallel, an issue with traditional recurrent models. Further attempts at leveraging advantages from both paradigms (Lieber et al., 2024; De et al., 2024; Dong et al., 2025) has also garnered interest. Nevertheless, these works fail to resolve existing criticisms regarding the use of context and properly integrating such models with retrieval-based techniques.

Retrieval-Augmented Generation. RAG-based methods augment the input of a LM with passages retrieved from an outside source (Gua et al., 2020; Lewis et al., 2020). Such methods have significantly improved performance on knowledge-intensive tasks, where the amount of information necessary for strong performance is difficult to store explicitly within parametric knowledge (Roberts et al., 2020). Further improvements have come under the form of improved filtering of retrieved passages (Asai et al., 2024), robustness to irrelevant passages (Yoran et al., 2024; Xu et al., 2024) or tuning of more components (Lin et al., 2024). However, RAG is not directly applicable for learning from contexts, as such methods do not search within the input-specific query but rather from an external database, nor do they account for the information bottleneck with LRMs. As such, we propose RESONA as a method to overcome these limitations.

Do LRMs Use Context Effectively? Despite their practical benefits, questions have arisen regarding the ability of LRMs to learn from input contexts (Akyürek et al., 2024). Jelassi et al. (2024) show that they struggle to directly copy information from contexts due to their fixed-sized latent state. Park et al. (2024) further show that they can struggle at retrieval-based (Arora et al., 2024) in-context learning, only solving such tasks through the addition of attention. Such observations have extended to real-world data, where LRMs have been shown to exhibit similar difficulties as Transformer LLMs (Huang, 2025; Liu et al., 2024) for long contexts (Ivgy et al., 2023; Hsieh et al., 2024). Accordingly, we introduce RESONA as a potential solution by as a way of providing additional information flow paths from the context to the generated input, enabling better utilization of the context for problem-solving.

Memory-enhanced Transformer. Due to the quadratic complexity of self-attention, transformer models face significant computational challenges when processing long inputs. Numerous approaches have been proposed to enhance transformers for long sequential data, often incorporating memory mechanisms or retrieval modules. Dai et al. (2019); Munkhdalai et al. (2024) segment long inputs into shorter sequences and process them recurrently. Mohtashami and Jaggi (2023) appends landmark tokens to represent each block of input and uses group attention to select relevant information. Borgeaud et al. (2022) enhances transformer performance with external data by leveraging a separated retriever module. Nunez et al. (2024) develop a Span-Expanded Attention for the hybridized attention model to retrieve the most relevant block and integrates it with the recent context for attention computation. However, it remains unclear whether and how retrieval-based modules can enhance the performance of generalized linear recurrent models such as GLA (Yang et al., 2024a), Mamba (Gu and Dao (2024); Dao and Gu (2024)), RWKV (Peng et al. (2023)), and DeltaNet (Yang et al. (2024b)).

3 RESONA

We introduce RESONA (Figure 2 and Algorithm 1) as a framework to enhance the context-copying abilities of LRMs through retrieval, without sacrificing original performance and versatility. Our end-to-end training enables models to utilize the context as a retrieval base from which information can be extracted, enabling the model to overcome the fixed-size latent space bottleneck and integrate information from the context directly into the hidden state. This is in contrast to traditional LRMs, where the information from the context must flow through the hidden state.

Algorithm 1 RESONA Algorithm.**Require:** Model \mathcal{M}

- 1: **Input:** Input $s \in \mathbb{R}^T$ and LRM hidden state $h \in \mathbb{R}^{L \times T \times H}$, **Output:** $y \in \mathbb{R}^{T \times D}$
- 2: Embed sequence s into $x \in \mathbb{R}^{T \times D}$.
- 3: **for** $l \leftarrow 1$ to L **do**
- 4: **if** Layer l is an RESONA layer **then**
- 5: $h_l, y^m = \mathcal{M}_l^{\text{LRM}}(x, h_l)$
- 6: $M = \mathcal{M}_l^{\text{C-and-S}}(x, h_l)$
- 7: $y^r = \mathcal{M}_l^{\text{KI}}(x, h_l, M)$
- 8: $\alpha = f(x)$
- 9: $y = \alpha \cdot y^m + (1 - \alpha)y^r$
- 10: **else**
- 11: $h_l, y = \mathcal{M}_l(x, h_l)$
- 12: $x = y$
- 13: **return** y

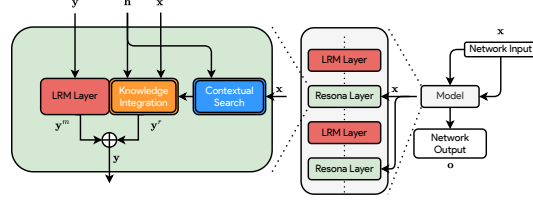


Figure 2: Primary components of RESONA: 1) **Contextual Search** which searches the context for relevant information and 2) **Knowledge Integration** which re-integrates the retrieved information into the model state. These enable information from the original network input to flow to arbitrary depths in the model, overcoming information decay within the model.

3.1 Problem Formulation and Overview

Let \mathbb{V} be a vocabulary of size V . A model \mathcal{M} applies a function $f : \mathbb{V}^* \rightarrow \mathbb{V}^*$, which maps an input sequence of tokens to an output sequence y . We also refer to the input $x = [x_1, \dots, x_T]$ as the “prompt” to the model \mathcal{M} and of the output sequence $y = f(x)$ as the generated “answer”. Furthermore, a sequence-to-token mapping is a function $g : \mathbb{V}^* \rightarrow \mathbb{V}$ that defines f by auto-regressive inference. Namely, for every input sequence $x \in \mathbb{V}^*$, x_{i+j} is defined recursively as $x_{i+j} = g(x_1, \dots, x_{i+j-1})$ and $f(x) = (x_{i+1}, x_{i+2}, \dots)$.

A linear recurrent model (LRM) is defined by a state update rule $u : \mathcal{S} \times \mathbb{V} \rightarrow \mathcal{S}$ and an output function $r : \mathcal{S} \rightarrow \mathbb{V}$, where \mathcal{S} is a finite set of states. Let $s_0 \in \mathcal{S}$ be some initial state. Given some sequence x of length L , the state of the model at iteration i is denoted by $S_i(x_1, \dots, x_i)$ and the output token is denoted by $R_i(x_1, \dots, x_i)$. These are defined recursively as:

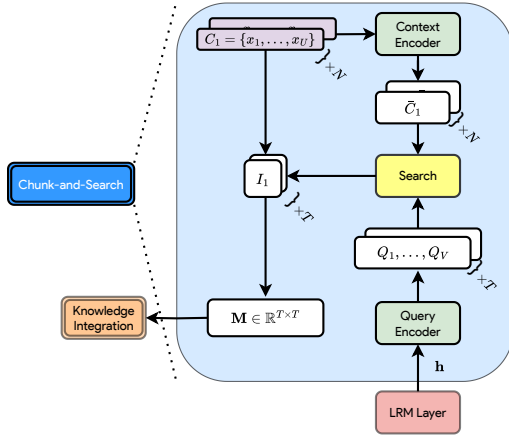
- 1) $S_0(\emptyset) = s_0$,
- 2) $h_i = S_i(x_1, \dots, x_i) = u(S_{i-1}(x_1, \dots, x_{i-1}), x_i)$,
- 3) $y_i = R_i(x_1, \dots, x_i) = r(S_i(x_1, \dots, x_i))$.

Information from x reaches y through a state $h \in \mathbb{R}^H$ where H is fixed and finite. Thus for increasing sequence length or information dense settings, such LRMs can struggle from the limited of h . This can be formalized more explicitly as

Lemma 3.1. *If $|\mathcal{S}| > 2^{H \times p}$, with p the precision of h , then h serves as an information bottleneck.*

Proof. Suppose r applies a different function on every state $s \in \mathcal{S}$. Then h needs to have the capacity to model every possible state s . If $|\mathcal{S}| > 2^{H \times p}$, then by consequence there must be a subset $S' \subseteq \mathcal{S}$ such that h represents at least 2 states s and s' with the same encoding. Suppose that no information is lost. Then this means that for any update rule u or r , applying these on s and s' has the same result. However, this means that s and s' are in fact the same state, hence there is no information loss by contradiction. \square

Thus we observe that the LRM is directly limited by the size of its hidden state, which can be insufficient for modeling more complex problems unless it grows with the size of the possible set of states. RESONA introduces two flexible components to overcome this constraint without sacrificing the primary benefits of LRMs (namely parallel training and inference time efficiency): 1) a **contextual search** operation that operates on the input to retrieve context-specific information and 2) a **knowledge integration** component that mixes the retrieved information with the LRM output.



Algorithm 2 Chunk-and-Search Algorithm.

Require: Context and Query Encoders \mathcal{C}, \mathcal{Q}

- 1: **Input:** Input $x \in \mathbb{R}^{T \times D}$ and LRM hidden state $h \in \mathbb{R}^{T \times H}$, **Output:** Attention mask $M \in \mathbb{R}^{T \times T}$
 - 2: Chunk x into $x' \in \mathbb{R}^{N \times U \times D}$
 - 3: Use \mathcal{C} to encode each context chunk x' into context embeddings $\tilde{C} \in \mathbb{R}^{N \times U \times E}$
 - 4: Use \mathcal{Q} to encode h into query embeddings $\tilde{Q} \in \mathbb{R}^{T \times E}$.
 - 5: Compute chunk index sets for each \tilde{Q}_j : $\{I_j\}_{j=1}^T = \{\text{Top-}k(\tilde{Q}_j, \tilde{C})\}_{j=1}^T$
 - 6: With $\{I_j\}_{j=1}^T$, compute a mask $M \in \mathbb{R}^{T \times T}$ such that $M_{ji} = 1 \iff (i \in \{I_j\})$.
-

Figure 3: A breakdown of our Chunk-and-Search implementation. The initial input context is chunked while the hidden state of the LRM layer is used as a query. Corresponding indices are retrieved for each query, creating a mask that is used for Knowledge Integration.

Contextual Search. In order to retrieve relevant context, RESONA implements contextual search as a chunk-and-search mechanism (Algorithm 2). The initial input x is first split into N chunks, each consisting of U tokens, to create $x' \in \mathbb{R}^{N \times U \times D}$. First, each of these chunks C_i is encoded using a context encoder \mathcal{C} into a context embedding \tilde{C}_i . Simultaneously, the hidden state of the adjacent linear-recurrent layer $h \in \mathbb{R}^{T \times H}$, is used to encode a number of queries into query embeddings $\tilde{Q}_{1:T}$ using a query encoder \mathcal{Q} . For each query, we search for the top- k similar contexts using a cosine-similarity search, which produces chunk indices that we can then use to retrieve the relevant input token positions. These are used to create a mask, which is passed to the **Knowledge-Integration** module.

Knowledge Integration. To integrate knowledge from the retrieved chunks, RESONA does as follows (Figure 4 and Algorithm 3). The knowledge integration module is a cross-attention module that can directly integrate information from the initial embedding into the LRM layer representation. To do so, the queries Q are directly computed from the hidden state of the prior LRM layer¹, while the keys K and values V are computed directly from the input embeddings x that directly follow after the initial embedding matrix E . Within the cross-attention module, we use a mask computed from our **Chunk-and-Search** implementation of the contextual search. This ensures that the cross attention module can mix in only the most relevant information from the input back into the cross-attention module, producing an output $y^r \in \mathbb{R}^{T \times D}$, which is then integrated with the output of the adjacent LRM layer y^m , computed as

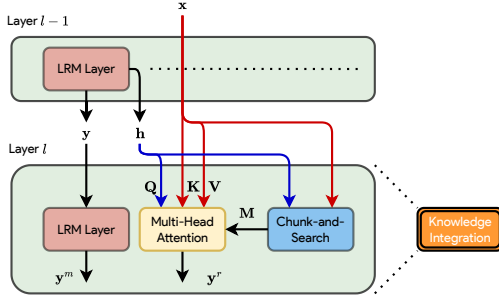
$$y = \alpha \cdot y^m + (1 - \alpha) \cdot y^r.$$

α can be computed on an input-dependent basis for each element of y or can alternatively be set as fixed hyper-parameter value. Because only the chunk-and-search design, each query attends to at most kU elements from the initial input in k contiguous blocks, enabling us to compute y^r efficiently using existing sparse attention mechanisms.

3.2 Training and Inference

When training RESONA, an important consideration is the auto-regressive nature of the model that therefore requires a causal mask. Specific to our implementation, to maintain this during the parallel nature of training, we ensure that for the query at index i , only

¹In the event that the first layer is augmented with RESONA, the queries are generated directly from the initial embeddings.



Algorithm 3 Knowledge Integration.

Require: Attention weights W_Q, W_K, W_V and output weights W_{out}

- 1: **Input:** Input $x \in \mathbb{R}^{T \times D}$ and LRM hidden state $h \in \mathbb{R}^{T \times H}$, mask $M \in \mathbb{R}^{T \times T}$, **Output:** $y^r \in \mathbb{R}^{T \times D}$
 - 2: From h , compute queries $Q \in \mathbb{R}^{T \times d_k}$ using W_Q . In parallel, compute $K, V \in \mathbb{R}^{T \times d_k}$ from x with W_K, W_V .
 - 3: Compute multi-head attention output $O = \text{CrossAttn}(Q, K, V, M)$, where $O \in \mathbb{R}^{T \times d_k}$.
 - 4: Project O using W_{out} into $y^r \in \mathbb{R}^{T \times D}$.
-

Figure 4: Knowledge Integration portion of RESONA. The hidden state is used as a query while the initial network input is used as the query and keys. A mask constructed from the contextual search is used to determine which information needs to be mixed back into the LRM representation, which is then used to compute an attention output that is integrated into the adjacent LRM output.

chunks that solely contain information prior to this position in the input are considered within the **Chunk-and-Search** process. This ensures that the mask M allows no information from future tokens to a the representation from the past.

During inference, tokens are dynamically chunked based on a predefined size and embedded into a chunked cache in parallel with the main model’s embedding, introducing no extra latency. For long prompts, chunking is integrated into the pre-filling stage, aligning with the token embedding pipeline and minimizing computation overhead.

4 Experiments, Results and Analysis

4.1 Tasks and Datasets

To test our method, we evaluate RESONA on both a number of synthetic benchmarks as well as real-world language benchmarks. In Section 4, we explain the experimental setting as well as evaluation methods for each. For each setting, we report a standard baseline where a backbone model is not augmented with RESONA. These baselines vary based on which backbones are capable of adequately learning the task without RESONA.

4.2 Main Results

4.2.1 Results on Synthetic Benchmarks.

We first evaluate on **synthetic benchmarks**, which include the multi-query associative recall (MQAR) task (Arora et al., 2024) as well as the Mechanistic Architecture Design (MAD) suite of tasks (Poli et al., 2024). For each, we report accuracy on a held-out test set. Accuracy is reported as the number of examples where the entire output is correctly predicted. For these benchmarks, we initialize models from scratch and train them on the task of interest. In these settings, we use a 4 layer model with a vocabulary size of 8192. Each model a hidden size of 128 and a context chunk size of 64 for those augmented with RESONA using. Models are all trained on 20K examples and evaluated on 1K examples. Figure 5 and Table 1 demonstrate that augmentation with RESONA enables better performance across all baselines, some by wide margins. For example, baseline models are often able to perfectly solve the MQAR task for shorter sequence lengths or a smaller number of KV-pairs, but fail catastrophically upon increasing either of these values. RESONA overcomes this significantly, as seen by near perfect accuracy even as these values increase. Similarly, models can struggle at specific tasks within the MAD suite, but RESONA can boost these performances by significant margins on average. On tasks in which LRM models already exhibit strong performance,

no degradation is observed through the addition of RESONA, highlighting its flexibility. We observe that this is consistent across multiple models (Poli et al., 2023; Fu et al., 2023), which are incapable of learning on some of the simpler settings but upon the addition of RESONA layers are able of maintaining nearly perfect accuracy for arbitrarily long sequences, showcasing its specific benefits in context-recall intensive settings.

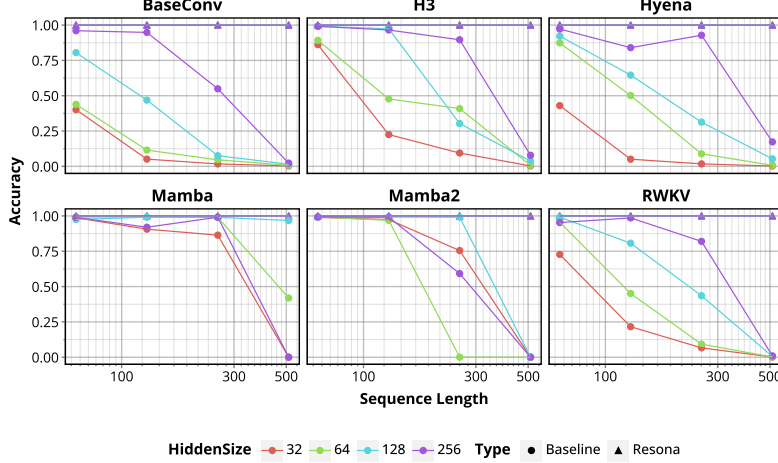


Figure 5: Results on MQAR tasks on varying sequence lengths. Baseline models remain limited in their ability to model increasingly long sequences even with increasing hidden size, whereas augmentation with RESONA perfect performance on arbitrary lengths.

Model	Compression	ICR	Noisy ICR	Fuzzy ICR	SC	Memorization	Average
MAMBA	38.3	76.7	74.9	9.3	33.2	88.5	53.5
w/ RESONA	38.2 (↓ 0.1)	99.9 (↑ 23.2)	100.0 (↑ 25.1)	63.4 (↑ 54.1)	42.7 (↑ 9.5)	88.8 (↑ 0.3)	72.1 (↑ 18.6)
MAMBA2	43.6	96.4	96.7	21.1	93.3	86.9	73.0
w/ RESONA	46.6 (↑ 3.0)	100.0 (↑ 3.6)	100.0 (↑ 3.3)	62.9 (↑ 41.8)	93.6 (↑ 0.3)	88.1 (↑ 1.2)	81.9 (↑ 8.9)
RWKV5	36.8	96.4	96.6	12.1	52.7	55.0	58.3
w/ RESONA	40.4 (↑ 3.6)	99.7 (↑ 3.3)	99.8 (↑ 3.2)	59.7 (↑ 47.6)	58.0 (↑ 5.3)	70.6 (↑ 15.6)	71.5 (↑ 13.2)
HYENA	42.2	79.3	77.4	9.96	72.8	88.9	61.7
w/ RESONA	42.6 (↑ 0.4)	99.9 (↑ 20.6)	99.9 (↑ 22.5)	66.2 (↑ 56.2)	74.3 (↑ 1.5)	89.0 (↑ 0.1)	78.7 (↑ 17.0)

Table 1: Performance on synthetic MAD (Poli et al., 2024) tasks. The best result for each metric is highlighted in bold. RESONA consistently boosts retrieval performance and shows gains even on compression and memorization tasks.

4.2.2 Language Modeling

To assess language modeling, we compare a baseline models with one augmented with RESONA layers. Here, we train on the WIKITEXT-103 dataset (Merity et al., 2016). In order to train models augmented with RESONA, we also augment the dataset. Specifically, we first consolidate all samples from the same Wikipedia entry into single sample, eliminating excessively short title lines or empty lines. We then use a LLaMA3.1-70B (Grattafiori et al., 2024) model to augment each sample such that we can make use of the RESONA retrieval mechanism. We then conduct the Chunk-and-Search process offline to create masks, in order to save computation during training. To account for the additional parameters introduced by RESONA, we present results in the baseline settings for two version, one where each LRM layer matches exactly that of the augmented model as well as a version where the hidden size of the layer has been increased to match the parameter count of the augmented counterpart. Evaluation results in Table 2 demonstrate the effectiveness of integrating RESONA consistently achieve lower perplexity than both their baseline counterparts and parameter-aligned variants, highlighting the general applicability of RESONA for language modeling. Notably, in the last row, modifying Hymba’s sliding window mask to our retrieve-

lead mask significantly improves performance, further underscoring its advantage over fixed sliding window masking.

4.2.3 Direct Fine-Tuning

To understand how well the addition of RESONA modules can improve performance on context-dependent tasks, we make use of pre-trained models in which we insert RESONA layers. The models are then fine-tuned directly, as described in Section 4.1, and we record performance using task-specific metrics. Due to some computational limitations, we provide results only for models where the baseline model is capable of performance above random on all benchmarks. In these settings, we choose 3 layers of the model to augment with RESONA. The models are then tuned using the corresponding training dataset of the task, before being tested on a held-out test set.

Model	Param	PPL
GLA	131M	14.265
GLA (same param)	142M	14.223
GLA+RESONA	145M	13.892
DELTA _{NET}	131M	13.044
DELTA _{NET} (same param)	142M	12.946
Delta _{Net} +RESONA	145M	12.541
RET _{NET}	132M	15.471
RET _{NET} (same param)	146M	15.431
RET _{NET} +RESONA	142M	14.742
MAMBA	140M	16.261
MAMBA (same param)	157M	16.173
MAMBA+RESONA	154M	15.943
HYMBA(64)	133M	16.688
HYMBA+RESONA(same param)	135M	15.887

Under this direct-fine-tuning setting, we evaluate on question answering benchmarks including NARRATIVEQA (Kociský et al., 2018), the Conversational Question Answering (COQA) challenge (Reddy et al., 2019) and TRIVIAQA (Joshi et al., 2017). For each task, we report results in terms of BLEU, ROUGE-L, Meteor (Banerjee and Lavie, 2005) and F1 scores. Table 3 presents these results, where we can observe improvements on both pre-trained MAMBA and HYMBA (with a sliding window of 256) models through the addition of RESONA layers. This is particularly evident with improvements across all metrics for all datasets, showing the general benefits that RESONA provides towards better context-dependent reasoning skills.

Model	TRIVIAQA				COQA				NARRATIVEQA			
	BLEU	ROUGE-L	METEOR	F1	BLEU	ROUGE-L	METEOR	F1	BLEU	ROUGE-L	METEOR	F1
MAMBA	28.3	66.0	44.8	40.2	35.5	73.0	49.3	60.6	12.6	47.0	34.7	34.7
W/ RESONA	30.7	68.0	45.6	41.8	44.3	75.0	52.2	61.2	13.2	50.0	36.9	36.2
HYMBA(256)	15.3	58.0	41.4	34.3	31.8	62.0	42.1	50.0	10.7	39.0	29.1	28.4
W/ RESONA	25.6	61.0	43.4	41.5	36.5	69.0	48.8	57.2	13.1	46.0	33.9	35.1
HYMBA	16.5	64.0	44.8	36.9	40.0	77.0	53.3	63.1	20.5	59.0	44.2	43.1
W/ RESONA	29.3	69.0	48.4	45.4	51.7	82.0	59.3	68.9	20.9	60.0	45.2	44.0

Table 3: Results on QA benchmarks, where augmentation with RESONA improves performance over all evaluation metrics. HYMBA indicates RESONA is added as a third branch with both the Hymba’s original linear and attention branches, while HYMBA(256) indicates where we reduce the window size of Hymba SWA from 1024 to 256, in order to create a fair comparison with our chunk size of 256.

5 Analysis and Discussion

5.1 RESONA VS RAG-like methods.

A natural comparison to make with RESONA is typical RAG-like methods, which append the retrieved passages directly to the input prior to applying the model. To compare with such methods, we design the following methods with RESONA: **1)** Using the input context directly as the data-store from which a pre-trained retriever can retrieve passages directly that are used as context (RETRIEVAL) and **2)** we remove the Knowledge Integration component and instead directly append all (decoded) retrieved passages from the Chunk-and-Search procedure to the initial input (RAG). Table 4 shows these results on a Hymba model, again on the tested QA datasets. The RESONA-augmented variant remains significantly more

Model	TRIVIAQA				CoQA				NARRATIVEQA			
	BLEU	ROUGE-L	METEOR	F1	BLEU	ROUGE-L	METEOR	F1	BLEU	ROUGE-L	METEOR	F1
HYMBA	15.3	58.0	41.4	34.3	31.8	62.0	42.1	50.0	10.7	39.0	29.1	28.4
W/RETRIEVAL	2.9	57.0	39.0	33.9	4.6	52.0	38.2	41.3	3.9	36.0	30.8	27.6
W/RAG	12.9	66.0	46.0	38.8	23.2	67.0	47.9	54.5	12.5	49.0	38.4	35.2
W/RESONA	25.6	61.0	43.4	41.5	36.5	69.0	48.8	57.2	13.1	46.0	33.9	35.1

Table 4: Performance comparison of HYMBA (256 window size), its RESONA-enhanced variants and two different RAG-style input.

performant than the other alternatives, demonstrating the benefits that acting directly on the representations can have.

5.2 Relationship with Hybrid Methods

Some previous works have suggested methods that enable linear recurrent models to improve their in-context learning abilities. Park et al. (2024) introduce a MAMBAFORMER architecture which interleaves self-attention and MAMBA layers, improving the ability to learn in-context on tasks in which pure MAMBA models struggle. Similarly, RESONA can be interpreted as a form of hybrid mixture of attention and recurrence, similar to Dong et al. (2025), with the difference lying in the frequency of attention and its sparsity within different layers. To better compare these two methods, we provide an ablation (Table 5) where we replace HYMBA layers with RESONA.

In this setting, 3 consecutive layers are trained in either setup. We observe a meaningful increase in performance on CoQA, indicating that for such types of tasks, the mechanism presented by RESONA could be more robust and suitable on a number of real world tasks.

5.3 Ablating on the position of layers.

By its nature, a natural question that emerges relates to the ease and effectiveness of determining the layers at which RESONA augmentations need to be made. The same results (Table 5) show that the placement of the 3 RESONA layers do not have a significant impact on the performance improvement relative to the baseline, which can be improved upon in nearly all ways in which the layers are selected. This highlights a level of robustness of the framework and method, hinting towards an ability to be used for a variety of additional tasks.

Model	Layer	CoQA			
		BLEU	ROUGE-L	METEOR	F1
HYMBA	0	31.8	62.0	42.1	50.0
W/RESONA		36.5	69.0	48.8	57.2
HYMBA	8	25.1	62.0	42.5	48.8
W/RESONA		41.2	73.0	51.5	61.4
HYMBA	15	21.8	60.0	41.5	48.0
W/RESONA		37.1	70.0	48.9	57.7
HYMBA	23	5.9	41.0	27.8	32.3
W/RESONA		29.1	62.0	42.8	50.1
HYMBA	29	5.8	40.0	27.6	30.3
W/RESONA		31.2	57.0	39.2	44.5

Table 5: A comparison of RESONA and HYMBA (Dong et al., 2025). Three consecutive layers are un-frozen for fine-tuning. In the RESONA-augmented setup, the attention branch of the selected layers is modified to the RESONA retrieval mechanism. A sliding window size of 256 is used while the corresponding number indicates the start index of the replaced layers.

6 Conclusion

In this work, we propose RESONA, a lightweight retrieval-based knowledge integration mechanism that significantly improves the ability of LRMs to use example-specific context. RESONA utilizes a novel mechanism to use the input-context as a retrieval data-store and integrate such information with the input during training and inference, enabling models to use it more effectively and overcome information bottleneck concerns. Across a number of both synthetic and real-world datasets, LRMs augmented with RESONA demonstrate significant performance gains compared to their base counterparts, demonstrating its ability to function as a general method applicable to broader scenarios.

References

- E. Akyürek, B. Wang, Y. Kim, and J. Andreas. In-context language learning: Architectures and algorithms. In *Forty-first International Conference on Machine Learning, ICML 2024, Vienna, Austria, July 21-27, 2024*. OpenReview.net, 2024. URL <https://openreview.net/forum?id=3Z9CRr5srl>.
- S. Arora, S. Eyuboglu, A. Timalsina, I. Johnson, M. Poli, J. Zou, A. Rudra, and C. Ré. Zoology: Measuring and improving recall in efficient language models. In *The Twelfth International Conference on Learning Representations, ICLR 2024, Vienna, Austria, May 7-11, 2024*. OpenReview.net, 2024. URL <https://openreview.net/forum?id=LY3ukUANKo>.
- A. Asai, Z. Wu, Y. Wang, A. Sil, and H. Hajishirzi. Self-rag: Learning to retrieve, generate, and critique through self-reflection. In *The Twelfth International Conference on Learning Representations, ICLR 2024, Vienna, Austria, May 7-11, 2024*. OpenReview.net, 2024. URL <https://openreview.net/forum?id=hSyW5go0v8>.
- D. Bahdanau, K. Cho, and Y. Bengio. Neural machine translation by jointly learning to align and translate. In Y. Bengio and Y. LeCun, editors, *3rd International Conference on Learning Representations, ICLR 2015, San Diego, CA, USA, May 7-9, 2015, Conference Track Proceedings*, 2015. URL <http://arxiv.org/abs/1409.0473>.
- S. Banerjee and A. Lavie. METEOR: an automatic metric for MT evaluation with improved correlation with human judgments. In J. Goldstein, A. Lavie, C. Lin, and C. R. Voss, editors, *Proceedings of the Workshop on Intrinsic and Extrinsic Evaluation Measures for Machine Translation and/or Summarization@ACL 2005, Ann Arbor, Michigan, USA, June 29, 2005*, pages 65–72. Association for Computational Linguistics, 2005. URL <https://aclanthology.org/W05-0909/>.
- M. Beck, K. Pöppel, M. Spanring, A. Auer, O. Prudnikova, M. Kopp, G. Klambauer, J. Brandstetter, and S. Hochreiter. xlm: Extended long short-term memory. In *Advances in Neural Information Processing Systems 38: Annual Conference on Neural Information Processing Systems 2024, December 10-15, 2024, Vancouver, Canada*, pages 5998–6008, 2017.
- S. Borgeaud, A. Mensch, J. Hoffmann, T. Cai, E. Rutherford, K. Millican, G. van den Driessche, J. Lespiau, B. Damoc, A. Clark, D. de Las Casas, A. Guy, J. Menick, R. Ring, T. Hennigan, S. Huang, L. Maggiore, C. Jones, A. Cassirer, A. Brock, M. Paganini, G. Irving, O. Vinyals, S. Osindero, K. Simonyan, J. W. Rae, E. Elsen, and L. Sifre. Improving language models by retrieving from trillions of tokens. In K. Chaudhuri, S. Jegelka, L. Song, C. Szepesvári, G. Niu, and S. Sabato, editors, *International Conference on Machine Learning, ICML 2022, 17-23 July 2022, Baltimore, Maryland, USA*, volume 162 of *Proceedings of Machine Learning Research*, pages 2206–2240. PMLR, 2022. URL <https://proceedings.mlr.press/v162/borgeaud22a.html>.
- T. B. Brown, B. Mann, N. Ryder, M. Subbiah, J. Kaplan, P. Dhariwal, A. Neelakantan, P. Shyam, G. Sastry, A. Askell, S. Agarwal, A. Herbert-Voss, G. Krueger, T. Henighan, R. Child, A. Ramesh, D. M. Ziegler, J. Wu, C. Winter, C. Hesse, M. Chen, E. Sigler, M. Litwin, S. Gray, B. Chess, J. Clark, C. Berner, S. McCandlish, A. Radford, I. Sutskever, and D. Amodei. Language models are few-shot learners. In H. Larochelle, M. Ranzato, R. Hadsell, M. Balcan, and H. Lin, editors, *Advances in Neural Information Processing Systems 33: Annual Conference on Neural Information Processing Systems 2020, NeurIPS 2020, December 6-12, 2020, virtual*, 2020. URL <https://proceedings.neurips.cc/paper/2020/hash/1457c0d6bfc4967418bfb8ac142f64a-Abstract.html>.
- K. Cho, B. van Merriënboer, Ç. Gülçehre, D. Bahdanau, F. Bougares, H. Schwenk, and Y. Bengio. Learning phrase representations using RNN encoder-decoder for statistical machine translation. In A. Moschitti, B. Pang, and W. Daelemans, editors, *Proceedings of the 2014 Conference on Empirical Methods in Natural Language Processing, EMNLP 2014, October 25-29, 2014, Doha, Qatar, A meeting of SIGDAT, a Special Interest Group of the ACL*, pages 1724–1734. ACL, 2014. doi: 10.3115/V1/D14-1179. URL <https://doi.org/10.3115/V1/D14-1179>.

- H. W. Chung, L. Hou, S. Longpre, B. Zoph, Y. Tay, W. Fedus, Y. Li, X. Wang, M. Dehghani, S. Brahma, A. Webson, S. S. Gu, Z. Dai, M. Suzgun, X. Chen, A. Chowdhery, A. Castro-Ros, M. Pellat, K. Robinson, D. Valter, S. Narang, G. Mishra, A. Yu, V. Y. Zhao, Y. Huang, A. M. Dai, H. Yu, S. Petrov, E. H. Chi, J. Dean, J. Devlin, A. Roberts, D. Zhou, Q. V. Le, and J. Wei. Scaling instruction-finetuned language models. *Journal on Machine Learning Research*, 25: 70:1–70:53, 2024. URL <https://jmlr.org/papers/v25/23-0870.html>.
- Z. Dai, Z. Yang, Y. Yang, J. G. Carbonell, Q. V. Le, and R. Salakhutdinov. Transformer-xl: Attentive language models beyond a fixed-length context. In A. Korhonen, D. R. Traum, and L. Màrquez, editors, *Proceedings of the 57th Conference of the Association for Computational Linguistics, ACL 2019, Florence, Italy, July 28- August 2, 2019, Volume 1: Long Papers*, pages 2978–2988. Association for Computational Linguistics, 2019. doi: 10.18653/V1/P19-1285. URL <https://doi.org/10.18653/v1/p19-1285>.
- T. Dao and A. Gu. Transformers are ssms: Generalized models and efficient algorithms through structured state space duality. In *Forty-first International Conference on Machine Learning, ICML 2024, Vienna, Austria, July 21-27, 2024*. OpenReview.net, 2024. URL <https://openreview.net/forum?id=ztn8FCR1td>.
- T. Dao, D. Y. Fu, S. Ermon, A. Rudra, and C. Ré. Flashattention: Fast and memory-efficient exact attention with io-awareness. In S. Koyejo, S. Mohamed, A. Agarwal, D. Belgrave, K. Cho, and A. Oh, editors, *Advances in Neural Information Processing Systems 35: Annual Conference on Neural Information Processing Systems 2022, NeurIPS 2022, New Orleans, LA, USA, November 28 - December 9, 2022*, 2022. URL http://papers.nips.cc/paper_files/paper/2022/hash/67d57c32e20fd0a7a302cb81d36e40d5-Abstract-Conference.html.
- S. De, S. L. Smith, A. Fernando, A. Botev, G. Cristian-Muraru, A. Gu, R. Haroun, L. Berrada, Y. Chen, S. Srinivasan, G. Desjardins, A. Doucet, D. Budden, Y. W. Teh, R. Pascanu, N. D. Freitas, and C. Gulcehre. Griffin: Mixing gated linear recurrences with local attention for efficient language models, 2024. URL <https://arxiv.org/abs/2402.19427>.
- X. Dong, Y. Fu, S. Diao, W. Byeon, Z. Chen, A. S. Mahabaleshwarkar, S.-Y. Liu, M. V. Keirsbilck, M.-H. Chen, Y. Suhara, Y. Lin, J. Kautz, and P. Molchanov. Hymba: A hybrid-head architecture for small language models, 2025. URL <https://openreview.net/forum?id=A1ztozypga>.
- Y. Dubois, C. X. Li, R. Taori, T. Zhang, I. Gulrajani, J. Ba, C. Guestrin, P. Liang, and T. B. Hashimoto. AlpacaFarm: A simulation framework for methods that learn from human feedback. In A. Oh, T. Naumann, A. Globerson, K. Saenko, M. Hardt, and S. Levine, editors, *Advances in Neural Information Processing Systems 36: Annual Conference on Neural Information Processing Systems 2023, NeurIPS 2023, New Orleans, LA, USA, December 10 - 16, 2023*, 2023. URL http://papers.nips.cc/paper_files/paper/2023/hash/5fc47800ee5b30b8777fdd30abcaaf3b-Abstract-Conference.html.
- D. Y. Fu, T. Dao, K. K. Saab, A. W. Thomas, A. Rudra, and C. Ré. Hungry hungry hippos: Towards language modeling with state space models. In *The Eleventh International Conference on Learning Representations, ICLR 2023, Kigali, Rwanda, May 1-5, 2023*. OpenReview.net, 2023. URL <https://openreview.net/forum?id=COZDy0WYGg>.
- Gemma Team. Gemma 2: Improving open language models at a practical size, 2024. URL <https://arxiv.org/abs/2408.00118>.
- A. Grattafiori et al. The llama 3 herd of models, 2024. URL <https://arxiv.org/abs/2407.21783>.
- R. Grazzi, J. Siems, S. Schrod, T. Brox, and F. Hutter. Is mamba capable of in-context learning? In *Third International Conference on Automated Machine Learning, AutoML 2024, Paris, France, September 9-12, 2024*. OpenReview.net, 2024. URL <https://openreview.net/forum?id=rJhOG0P8nr>.
- A. Gu and T. Dao. Mamba: Linear-time sequence modeling with selective state spaces. In *First Conference on Language Modeling, COLM 2024, Philadelphia, PA, United States, October 7-9, 2024*. OpenReview.net, 2024. URL <https://openreview.net/forum?id=tEYskw1VY2>.

- A. Gu, K. Goel, and C. Ré. Efficiently modeling long sequences with structured state spaces. In *The Tenth International Conference on Learning Representations, ICLR 2022, Virtual Event, April 25-29, 2022*. OpenReview.net, 2022. URL <https://openreview.net/forum?id=uYLFoz1v1AC>.
- K. Guu, K. Lee, Z. Tung, P. Pasupat, and M. Chang. Retrieval augmented language model pre-training. In *Proceedings of the 37th International Conference on Machine Learning, ICML 2020, 13-18 July 2020, Virtual Event*, volume 119 of *Proceedings of Machine Learning Research*, pages 3929–3938. PMLR, 2020. URL <http://proceedings.mlr.press/v119/guu20a.html>.
- S. Hochreiter and J. Schmidhuber. Long short-term memory. *Neural Comput.*, 9(8):1735–1780, 1997. doi: 10.1162/NECO.1997.9.8.1735. URL <https://doi.org/10.1162/neco.1997.9.8.1735>.
- C. Hsieh, S. Sun, S. Krizan, S. Acharya, D. Rekesh, F. Jia, Y. Zhang, and B. Ginsburg. RULER: what’s the real context size of your long-context language models? In *First Conference on Language Modeling, COLM 2024, Philadelphia, PA, United States, October 7-9, 2024*. OpenReview.net, 2024. URL <https://openreview.net/forum?id=kIoBbc76Sy>.
- J. Huang. How well can a long sequence model model long sequences? comparing architectural inductive biases on long-context abilities. In *International Conference on Computational Linguistics, COLING 2025, January 19 – 24 2025, Abu Dhabi, UAE, 2025*.
- M. Ivgi, U. Shaham, and J. Berant. Efficient long-text understanding with short-text models. *Trans. Assoc. Comput. Linguistics*, 11:284–299, 2023. doi: 10.1162/TACL_A_00547. URL <https://doi.org/10.1162/tacl.a.00547>.
- S. Jelassi, D. Brandfonbrener, S. M. Kakade, and E. Malach. Repeat after me: Transformers are better than state space models at copying. In *Forty-first International Conference on Machine Learning, ICML 2024, Vienna, Austria, July 21-27, 2024*. OpenReview.net, 2024. URL <https://openreview.net/forum?id=duRROGeoQT>.
- M. Joshi, E. Choi, D. S. Weld, and L. Zettlemoyer. Triviaqa: A large scale distantly supervised challenge dataset for reading comprehension. In R. Barzilay and M. Kan, editors, *Proceedings of the 55th Annual Meeting of the Association for Computational Linguistics, ACL 2017, Vancouver, Canada, July 30 - August 4, Volume 1: Long Papers*, pages 1601–1611. Association for Computational Linguistics, 2017. doi: 10.18653/V1/P17-1147. URL <https://doi.org/10.18653/v1/P17-1147>.
- J. Kaplan, S. McCandlish, T. Henighan, T. B. Brown, B. Chess, R. Child, S. Gray, A. Radford, J. Wu, and D. Amodei. Scaling laws for neural language models, 2020. URL <https://arxiv.org/abs/2001.08361>.
- A. Katharopoulos, A. Vyas, N. Pappas, and F. Fleuret. Transformers are rnns: Fast autoregressive transformers with linear attention. In *Proceedings of the 37th International Conference on Machine Learning, ICML 2020, 13-18 July 2020, Virtual Event*, volume 119 of *Proceedings of Machine Learning Research*, pages 5156–5165. PMLR, 2020. URL <http://proceedings.mlr.press/v119/katharopoulos20a.html>.
- T. Kociský, J. Schwarz, P. Blunsom, C. Dyer, K. M. Hermann, G. Melis, and E. Grefenstette. The narrativeqa reading comprehension challenge. *Trans. Assoc. Comput. Linguistics*, 6:317–328, 2018. doi: 10.1162/TACL_A_00023. URL <https://doi.org/10.1162/tacl.a.00023>.
- P. S. H. Lewis, E. Perez, A. Piktus, F. Petroni, V. Karpukhin, N. Goyal, H. Küttler, M. Lewis, W. Yih, T. Rocktäschel, S. Riedel, and D. Kiela. Retrieval-augmented generation for knowledge-intensive NLP tasks. In H. Larochelle, M. Ranzato, R. Hadsell, M. Balcan, and H. Lin, editors, *Advances in Neural Information Processing Systems 33: Annual Conference on Neural Information Processing Systems 2020, NeurIPS 2020, December 6-12, 2020, virtual*, 2020. URL <https://proceedings.neurips.cc/paper/2020/hash/6b493230205f780e1bc26945df7481e5-Abstract.html>.

- O. Lieber, B. Lenz, H. Bata, G. Cohen, J. Osin, I. Dalmedigos, E. Safahi, S. Meirom, Y. Belinkov, S. Shalev-Shwartz, O. Abend, R. Alon, T. Asida, A. Bergman, R. Glozman, M. Gokhman, A. Manevich, N. Ratner, N. Rozen, E. Shwartz, M. Zusman, and Y. Shoham. Jamba: A hybrid transformer-mamba language model, 2024. URL <https://arxiv.org/abs/2403.19887>.
- X. V. Lin, X. Chen, M. Chen, W. Shi, M. Lomeli, R. James, P. Rodriguez, J. Kahn, G. Szilvasy, M. Lewis, L. Zettlemoyer, and W. Yih. RA-DIT: retrieval-augmented dual instruction tuning. In *The Twelfth International Conference on Learning Representations, ICLR 2024, Vienna, Austria, May 7-11, 2024*. OpenReview.net, 2024. URL <https://openreview.net/forum?id=220Tbutug9>.
- N. F. Liu, K. Lin, J. Hewitt, A. Paranjape, M. Bevilacqua, F. Petroni, and P. Liang. Lost in the middle: How language models use long contexts. *Trans. Assoc. Comput. Linguistics*, 12:157–173, 2024. doi: 10.1162/TACL\A\00638. URL <https://doi.org/10.1162/tacl.a.00638>.
- S. Merity, C. Xiong, J. Bradbury, and R. Socher. Pointer sentinel mixture models, 2016.
- A. Mohtashami and M. Jaggi. Landmark attention: Random-access infinite context length for transformers. *CoRR*, abs/2305.16300, 2023. doi: 10.48550/ARXIV.2305.16300. URL <https://doi.org/10.48550/arXiv.2305.16300>.
- T. Munkhdalai, M. Faruqui, and S. Gopal. Leave no context behind: Efficient infinite context transformers with infini-attention. *CoRR*, abs/2404.07143, 2024. doi: 10.48550/ARXIV.2404.07143. URL <https://doi.org/10.48550/arXiv.2404.07143>.
- E. Nunez, L. Zancato, B. Bowman, A. Golatkar, W. Xia, and S. Soatto. Expansion span: Combining fading memory and retrieval in hybrid state space models. *CoRR*, abs/2412.13328, 2024. doi: 10.48550/ARXIV.2412.13328. URL <https://doi.org/10.48550/arXiv.2412.13328>.
- OpenAI. Gpt-4 technical report, 2024. URL <https://arxiv.org/abs/2303.08774>.
- A. Orvieto, S. L. Smith, A. Gu, A. Fernando, Ç. Gülçehre, R. Pascanu, and S. De. Resurrecting recurrent neural networks for long sequences. In A. Krause, E. Brunskill, K. Cho, B. Engelhardt, S. Sabato, and J. Scarlett, editors, *International Conference on Machine Learning, ICML 2023, 23-29 July 2023, Honolulu, Hawaii, USA*, volume 202 of *Proceedings of Machine Learning Research*, pages 26670–26698. PMLR, 2023. URL <https://proceedings.mlr.press/v202/orvieto23a.html>.
- L. Ouyang, J. Wu, X. Jiang, D. Almeida, C. L. Wainwright, P. Mishkin, C. Zhang, S. Agarwal, K. Slama, A. Ray, J. Schulman, J. Hilton, F. Kelton, L. Miller, M. Simens, A. Askell, P. Welinder, P. F. Christiano, J. Leike, and R. Lowe. Training language models to follow instructions with human feedback. In S. Koyejo, S. Mohamed, A. Agarwal, D. Belgrave, K. Cho, and A. Oh, editors, *Advances in Neural Information Processing Systems 35: Annual Conference on Neural Information Processing Systems 2022, NeurIPS 2022, New Orleans, LA, USA, November 28 - December 9, 2022*, 2022. URL http://papers.nips.cc/paper_files/paper/2022/hash/b1efde53be364a73914f58805a001731-Abstract-Conference.html.
- J. Park, J. Park, Z. Xiong, N. Lee, J. Cho, S. Oymak, K. Lee, and D. Papailiopoulos. Can mamba learn how to learn? A comparative study on in-context learning tasks. In *Forty-first International Conference on Machine Learning, ICML 2024, Vienna, Austria, July 21-27, 2024*. OpenReview.net, 2024. URL <https://openreview.net/forum?id=GbFluKMmtE>.
- B. Peng, E. Alcaide, Q. Anthony, A. Albalak, S. Arcadinho, S. Biderman, H. Cao, X. Cheng, M. Chung, L. Derczynski, X. Du, M. Grella, K. K. GV, X. He, H. Hou, P. Kazienko, J. Kocon, J. Kong, B. Koptyra, H. Lau, J. Lin, K. S. I. Mantri, F. Mom, A. Saito, G. Song, X. Tang, J. S. Wind, S. Wozniak, Z. Zhang, Q. Zhou, J. Zhu, and R. Zhu. RWKV: reinventing rnns for the transformer era. In H. Bouamor, J. Pino, and K. Bali, editors, *Findings of the Association for Computational Linguistics: EMNLP 2023, Singapore, December 6-10, 2023*, pages 14048–14077. Association for Computational Linguistics, 2023. doi: 10.18653/V1/2023.FINDINGS-EMNLP.936. URL <https://doi.org/10.18653/v1/2023.findings-emnlp.936>.

- B. Peng, D. Goldstein, Q. Anthony, A. Albalak, E. Alcaide, S. Biderman, E. Cheah, X. Du, T. Ferdinan, H. Hou, P. Kazienko, K. K. GV, J. Kocon, B. Koptyra, S. Krishna, R. M. Jr., N. Muennighoff, F. Obeid, A. Saito, G. Song, H. Tu, S. Wozniak, R. Zhang, B. Zhao, Q. Zhao, P. Zhou, J. Zhu, and R. Zhu. Eagle and finch: RWKV with matrix-valued states and dynamic recurrence. In *First Conference on Language Modeling, COLM 2024, Philadelphia, PA, United States, October 7-9, 2024*. OpenReview.net, 2024. URL <https://openreview.net/forum?id=soz1SEiPeq>.
- M. Poli, S. Massaroli, E. Nguyen, D. Y. Fu, T. Dao, S. Baccus, Y. Bengio, S. Ermon, and C. Ré. Hyena hierarchy: Towards larger convolutional language models. In A. Krause, E. Brunskill, K. Cho, B. Engelhardt, S. Sabato, and J. Scarlett, editors, *International Conference on Machine Learning, ICML 2023, 23-29 July 2023, Honolulu, Hawaii, USA*, volume 202 of *Proceedings of Machine Learning Research*, pages 28043–28078. PMLR, 2023. URL <https://proceedings.mlr.press/v202/poli23a.html>.
- M. Poli, A. W. Thomas, E. Nguyen, P. Ponnusamy, B. Deiseroth, K. Kersting, T. Suzuki, B. Hie, S. Ermon, C. Ré, C. Zhang, and S. Massaroli. Mechanistic design and scaling of hybrid architectures. In *Forty-first International Conference on Machine Learning, ICML 2024, Vienna, Austria, July 21-27, 2024*. OpenReview.net, 2024. URL <https://openreview.net/forum?id=GDp7Gyd9nf>.
- Z. Qin, S. Yang, and Y. Zhong. Hierarchically gated recurrent neural network for sequence modeling. In A. Oh, T. Naumann, A. Globerson, K. Saenko, M. Hardt, and S. Levine, editors, *Advances in Neural Information Processing Systems 36: Annual Conference on Neural Information Processing Systems 2023, NeurIPS 2023, New Orleans, LA, USA, December 10 - 16, 2023*, 2023. URL http://papers.nips.cc/paper_files/paper/2023/hash/694be3548697e9cc8999d45e8d16fe1e-Abstract-Conference.html.
- Qwen. Qwen2.5 technical report, 2024. URL <https://arxiv.org/abs/2412.15115>.
- S. Reddy, D. Chen, and C. D. Manning. Coqa: A conversational question answering challenge. *Trans. Assoc. Comput. Linguistics*, 7:249–266, 2019. doi: 10.1162/TACL\A\00266. URL <https://doi.org/10.1162/tacl.a.00266>.
- A. Roberts, C. Raffel, and N. Shazeer. How much knowledge can you pack into the parameters of a language model? In B. Webber, T. Cohn, Y. He, and Y. Liu, editors, *Proceedings of the 2020 Conference on Empirical Methods in Natural Language Processing, EMNLP 2020, Online, November 16-20, 2020*, pages 5418–5426. Association for Computational Linguistics, 2020. doi: 10.18653/V1/2020.EMNLP-MAIN.437. URL <https://doi.org/10.18653/v1/2020.emnlp-main.437>.
- D. E. Rumelhart. *Parallel distributed processing, 9th Edition*. MIT Pr., 1989. ISBN 026268053X. URL <https://www.worldcat.org/oclc/60445750>.
- Y. Sun, X. Li, K. Dalal, J. Xu, A. Vikram, G. Zhang, Y. Dubois, X. Chen, X. Wang, S. Koyejo, T. Hashimoto, and C. Guestrin. Learning to (learn at test time): Rnns with expressive hidden states, 2024. URL <https://arxiv.org/abs/2407.04620>.
- A. Vaswani, N. Shazeer, N. Parmar, J. Uszkoreit, L. Jones, A. N. Gomez, L. Kaiser, and I. Polosukhin. Attention is all you need. In I. Guyon, U. von Luxburg, S. Bengio, H. M. Wallach, R. Fergus, S. V. N. Vishwanathan, and R. Garnett, editors, *Advances in Neural Information Processing Systems 30: Annual Conference on Neural Information Processing Systems 2017, December 4-9, 2017, Long Beach, CA, USA*, pages 5998–6008, 2017. URL <https://proceedings.neurips.cc/paper/2017/hash/3f5ee243547dee91fbd053c1c4a845aa-Abstract.html>.
- F. Xu, W. Shi, and E. Choi. RECOMP: improving retrieval-augmented lms with context compression and selective augmentation. In *The Twelfth International Conference on Learning Representations, ICLR 2024, Vienna, Austria, May 7-11, 2024*. OpenReview.net, 2024. URL <https://openreview.net/forum?id=mlJLVigNhp>.
- S. Yang and Y. Zhang. Fla: A triton-based library for hardware-efficient implementations of linear attention mechanism, Jan. 2024. URL <https://github.com/fla-org/flash-linear-attention>.

- S. Yang, B. Wang, Y. Shen, R. Panda, and Y. Kim. Gated linear attention transformers with hardware-efficient training. In *Forty-first International Conference on Machine Learning, ICML 2024, Vienna, Austria, July 21-27, 2024*. OpenReview.net, 2024a. URL <https://openreview.net/forum?id=ia5XvxFUJT>.
- S. Yang, B. Wang, Y. Zhang, Y. Shen, and Y. Kim. Parallelizing linear transformers with the delta rule over sequence length. *CoRR*, abs/2406.06484, 2024b. doi: 10.48550/ARXIV.2406.06484. URL <https://doi.org/10.48550/arXiv.2406.06484>.
- S. Yang, J. Kautz, and A. Hatamizadeh. Gated delta networks: Improving mamba2 with delta rule. In *The Thirteenth International Conference on Learning Representations*, 2025. URL <https://openreview.net/forum?id=r8H7xhYPwz>.
- O. Yoran, T. Wolfson, O. Ram, and J. Berant. Making retrieval-augmented language models robust to irrelevant context. In *The Twelfth International Conference on Learning Representations, ICLR 2024, Vienna, Austria, May 7-11, 2024*. OpenReview.net, 2024. URL <https://openreview.net/forum?id=ZS4m74kZpH>.
- Y. Zhang, S. Yang, R.-J. Zhu, Y. Zhang, L. Cui, Y. Wang, B. Wang, F. Shi, B. Wang, W. Bi, P. Zhou, and G. Fu. Gated slot attention for efficient linear-time sequence modeling. In *Advances in Neural Information Processing Systems 38: Annual Conference on Neural Information Processing Systems 2024, NeurIPS 2024, December 10-15, 2024, Vancouver, BC, Canada*, 2024. URL <https://openreview.net/forum?id=jY4PhQibmg>.

A Details

A.1 Model Definitions

Let $\{(k_t, v_t)\}_{t=1}^L$ denote a sequence of key-value pairs with $k_t, v_t \in \mathbb{R}^d$, and let (k^*, v^*) be the target pair. We analyze three components:

- **Linear Recurrence:** The hidden state $S_t \in \mathbb{R}^{d \times d}$ in a linear recurrent model evolves as:

$$S_t = S_{t-1} + v_t k_t^\top, \quad S_0 = \mathbf{0}, \quad (1)$$

with output $o_{\text{linear}} = S_t q = \sum_{i=1}^t (k_i^\top q) v_i$.

- **Semantic Search:** A sentence transformer $f_\theta : \mathbb{R}^d \rightarrow \mathbb{R}^m$ retrieves top-C keys $K_{\text{ret}} = \{k_j\}_{j=1}^C$ via cosine similarity:

$$\cos(f_\theta(q), f_\theta(k_j)) = \frac{f_\theta(q)^\top f_\theta(k_j)}{\|f_\theta(q)\|_2 \|f_\theta(k_j)\|_2}. \quad (2)$$

- **Hybrid Model:** Combines outputs via:

$$o_{\text{hybrid}} = \lambda o_{\text{linear}} + (1 - \lambda) o_{\text{attn}}, \quad \lambda \in [0, 1], \quad (3)$$

$$\text{where } o_{\text{attn}} = \sum_{j=1}^C \frac{\exp(q^\top k_j)}{\sum_{m=1}^C \exp(q^\top k_m)} v_j.$$

B Theoretical Background

B.1 Rank Limitation of Linear Recurrence

Lemma B.1 (Rank Bound). *For $L > d$, the hidden state $S_L = \sum_{t=1}^L v_t k_t^\top$ satisfies:*

$$\text{rank}(S_L) \leq d. \quad (4)$$

Proof. Each term $v_t k_t^\top$ is rank-1. The sum of L rank-1 matrices in $\mathbb{R}^{d \times d}$ cannot exceed rank d . \square

Corollary B.2 (Interference Error). *The linear model's retrieval error grows as:*

$$\mathcal{E}_{\text{linear}} = \|o_{\text{linear}} - v^*\|_2 \leq \|q\|_2 \sum_{i \neq *} \|k_i\|_2 \|v_i\|_2. \quad (5)$$

Proof. From $o_{\text{linear}} = \sum_{i=1}^L (k_i^\top q) v_i$, apply Cauchy-Schwarz: $\|\sum_{i \neq *} (k_i^\top q) v_i\|_2 \leq \|q\|_2 \sum_{i \neq *} \|k_i\|_2 \|v_i\|_2$. \square

C Additional Results

C.1 Detailed Pretraining Results

	Param	PPL	ARC Challenge		ARC Easy		HellaSwag		OpenBookQA		PIQA		PubMedQA	RACE	Winogrande	AVG
			Acc	Acc Norm	Acc	Acc Norm	Acc	Acc Norm	Acc	Acc Norm	Acc	Acc Norm	Acc	Acc	Acc	Acc
GLA	131M	14.265	0.1843	0.221	0.3683	0.3502	0.2671	0.2692	0.184	0.268	0.5392	0.5109	0.336	0.2364	0.5028	0.3259
GLA (same param)	142M	14.223	0.2073	0.2483	0.3409	0.3418	0.2701	0.2696	0.158	0.234	0.5321	0.5141	0.358	0.2478	0.4949	0.3243
GLA+RESONA	145M	13.892	0.192	0.2517	0.3405	0.3253	0.2646	0.2716	0.174	0.272	0.5457	0.5261	0.352	0.2469	0.5249	0.3297
DELTA.NET	131M	13.044	0.2201	0.2628	0.2849	0.2912	0.2613	0.2607	0.146	0.262	0.5234	0.5038	0.35	0.2545	0.5059	0.3174
DELTA.NET (same param)	142M	12.946	0.2159	0.256	0.3001	0.2845	0.2592	0.2635	0.178	0.278	0.5305	0.5125	0.34	0.266	0.4728	0.3199
DeltaNet+RESONA	145M	12.541	0.2073	0.2449	0.2963	0.2963	0.2686	0.2757	0.156	0.272	0.5419	0.5283	0.334	0.2517	0.5012	0.3210

Table 6: Detailed harness evaluation results from pre-training.

C.2 Detailed Supervised Fine-Tuning Results

Model	4K				8K				16K			
	Ver. 1	Ver. 2	Ver. 3	Multi-Value	Ver. 1	Ver. 2	Ver. 3	Multi-Value	Ver. 1	Ver. 2	Ver. 3	Multi-Value
MAMBA Baseline	5.00	1.80	0.75	0.898	0.65	0.45	0.15	0.458	0.00	0.35	0.20	0.494
MAMBA 20×lr	5.00	3.65	1.80	1.358	5.00	0.85	0.45	0.528	4.90	0.05	0.00	0.669
MAMBA 50×lr	5.00	3.00	1.10	1.267	4.95	0.60	0.20	0.533	4.00	0.05	0.00	0.550
DELTANET Baseline	2.15	2.95	1.45	1.301	1.90	1.45	0.70	0.321	1.00	0.25	0.00	0.883
DELTANET 20×lr	5.00	4.10	0.60	0.876	5.00	2.60	0.80	1.453	5.00	0.60	0.10	0.973
DELTANET 50×lr	5.00	4.40	1.45	1.676	5.00	1.25	0.35	1.312	5.00	0.45	0.05	0.885
GLA Baseline	2.90	3.65	0.05	1.389	0.25	0.55	0.00	0.846	0.00	0.05	0.00	0.291
GLA 20×lr	2.55	3.90	0.10	1.310	0.30	0.50	0.00	0.930	0.00	0.10	0.00	0.578
GLA 50×lr	3.00	3.85	0.15	1.353	0.20	0.60	0.00	0.900	0.00	0.05	0.00	0.657

Table 7: Results on Needle-in-a-Haystack (NIAH) using a haystack of varying sizes. Models are scored on performance on a continuous scale from 0 (worst) to 5 (best). In all settings, there is a single needle placed arbitrarily within the haystack. Different variants mean that the format of the needle or haystack changes, such as being a number, keyword or UUID sequence. Here $\alpha \times \text{lr}$ denotes RESONA is trained with a learning rate multiplied by α .

	ARC Challenge		ARC Easy		HellaSwag		OpenBookQA		PIQA		PubMedQA	RACE	Winogrande	AVG
	Acc	Acc Norm	Acc	Acc Norm	Acc	Acc Norm	Acc	Acc Norm	Acc	Acc Norm	Acc	Acc	Acc	
GLA	0.2381	0.2747	0.5442	0.5046	0.3852	0.4903	0.198	0.314	0.7008	0.7008	0.552	0.3110	0.5288	0.4417
GLA+RESONA	0.2466	0.2918	0.5497	0.5227	0.3738	0.4722	0.188	0.308	0.6944	0.7010	0.550	0.3139	0.5399	0.4424
DELTANET	0.2363	0.2637	0.5636	0.5341	0.3852	0.4893	0.198	0.316	0.7035	0.7002	0.552	0.3388	0.5375	0.4475
DELTANET+RESONA	0.2440	0.2722	0.5812	0.5455	0.3909	0.4982	0.198	0.314	0.7024	0.6997	0.556	0.3292	0.5375	0.4514
MAMBA	0.3558	0.3805	0.6953	0.6427	0.4958	0.6490	0.270	0.382	0.7535	0.7535	0.684	0.3598	0.6440	0.5435
MAMBA+RESONA	0.3823	0.3951	0.6907	0.6904	0.4804	0.6292	0.300	0.406	0.7372	0.7383	0.690	0.3445	0.6338	0.5475

Table 8: Detailed harness evaluation results from supervised fine-tuning of different pre-trained LRMs. After undergoing the same SFT as the backbone models, RESONA-enhanced models achieve comparable or superior zero-shot lm-harness evaluation scores to baselines. Combined with Table 7, these results demonstrate that the RESONA module enhances the backbone’s in-context learning (ICL) capability while maintaining its foundational language modeling performance.

C.3 Training Details for Synthetic Benchmarks

Multi-Query Associative Recall (MQAR). We evaluate RESONA on the MQAR task by training six base architectures: **Base Con**, **H3**, **Hyena**, **Mamba**, **Mamba2**, and **RWKV**. All models are trained with a 4-layer configuration and a hidden dimension (d_{model}) ranging from 32 to 256. The sequence lengths vary from 64 to 512, with the number of key-value (KV) pairs corresponding to 4–32, respectively. To integrate RESONA, we insert the **Resona Layer** into either the first or third layer of each model, using the same d_{model} settings. The learning rate is swept using the default settings from [Arora et al. \(2024\)](#). For the **Resona Layer**, we use a chunk size of 2 and a top- k value of 1. The exact results for each model, sequence length, and hidden dimension can be found in Table 9.

Mechanistic Architecture Design (MAD) Suite. For the MAD tasks, we adopt a 4-hybrid block configuration, where each block consists of a linear recurrent layer followed by a SwiGLU layer. We follow the benchmark settings from [Poli et al. \(2024\)](#), using a batch size of 128 and a learning rate range of 1e-3 to 1e-4. For the **Resona Layer**, we set the chunk size to 6 and the top- k value to 1.

C.4 Training Details for Real-World Tasks

Pretraining During pre-training, we prioritized maintaining consistent model depth across architectures. For GLA, DeltaNet, and RetNet, we adopted the architecture implementations from FLA-Hub ([Yang and Zhang, 2024](#)), configuring them with 24 layers and a hidden size of 600. For Hyamba, we utilized NVIDIA’s official 150M implementation (24 layers with a hidden size of 512). For Mamba, we employed FLA-Hub’s implementation with 48 layers and a hidden size of 600. For comparative models with equivalent parameter counts, we adjusted the hidden size from 600 to 640. Following the methodology outlined in the Hyamba paper, we integrated RESONA modules at the shallowest, middle, and deepest layers to reinforce critical information flow. Each model was trained for 8,000 steps, with model selection performed using a dedicated validation set. The training configuration employed

Model	Length=64				Length=128				Length=256				Length=512			
	KV Pairs				KV Pairs				KV Pairs				KV Pairs			
	32	64	128	256	32	64	128	256	32	64	128	256	32	64	128	256
BaseConv	0.401	0.439	0.805	0.960	0.051	0.115	0.469	0.948	0.017	0.046	0.076	0.549	0.003	0.007	0.015	0.023
BaseConv+RESONA0	1.000	1.000	1.000	1.000	1.000	1.000	1.000	1.000	1.000	1.000	1.000	1.000	1.000	1.000	1.000	1.000
BaseConv+RESONA2	1.000	1.000	1.000	1.000	1.000	1.000	1.000	1.000	1.000	1.000	1.000	1.000	1.000	1.000	1.000	1.000
H3	0.861	0.892	0.991	0.991	0.225	0.477	0.974	0.965	0.094	0.409	0.303	0.896	0.003	0.007	0.038	0.078
H3+RESONA0	1.000	1.000	1.000	1.000	1.000	1.000	1.000	1.000	1.000	1.000	1.000	1.000	1.000	1.000	1.000	1.000
H3+RESONA2	1.000	1.000	1.000	1.000	1.000	1.000	1.000	1.000	1.000	1.000	1.000	1.000	1.000	1.000	1.000	1.000
Hyena	0.430	0.874	0.922	0.972	0.051	0.501	0.646	0.840	0.018	0.089	0.313	0.928	0.002	0.007	0.053	0.173
Hyena+RESONA0	1.000	1.000	1.000	1.000	1.000	1.000	1.000	1.000	1.000	1.000	1.000	1.000	1.000	1.000	1.000	1.000
Hyena+RESONA2	1.000	1.000	1.000	1.000	1.000	1.000	1.000	1.000	1.000	1.000	1.000	1.000	1.000	1.000	1.000	1.000
RWKV	0.727	0.955	0.992	0.953	0.216	0.451	0.807	0.986	0.066	0.093	0.435	0.820	0.001	0.002	0.005	0.010
RWKV+RESONA0	1.000	1.000	1.000	1.000	1.000	1.000	1.000	1.000	1.000	1.000	1.000	1.000	1.000	1.000	1.000	1.000
RWKV+RESONA2	1.000	1.000	1.000	1.000	1.000	1.000	1.000	1.000	1.000	1.000	1.000	1.000	1.000	1.000	1.000	1.000
Mamba	0.987	0.992	0.975	0.990	0.906	0.992	0.991	0.920	0.864	0.990	0.990	0.991	0.000	0.419	0.968	0.000
Mamba+RESONA0	1.000	1.000	1.000	1.000	1.000	1.000	1.000	1.000	1.000	1.000	1.000	1.000	1.000	1.000	1.000	1.000
Mamba+RESONA2	1.000	1.000	1.000	1.000	1.000	1.000	1.000	1.000	1.000	1.000	1.000	1.000	1.000	1.000	1.000	1.000
Mamba2	0.990	0.992	0.991	0.993	0.974	0.969	0.992	0.991	0.755	0.000	0.991	0.592	0.000	0.000	0.001	0.000
Mamba2+RESONA0	1.000	1.000	1.000	1.000	1.000	1.000	1.000	1.000	1.000	1.000	1.000	1.000	1.000	1.000	1.000	1.000
Mamba2+RESONA2	1.000	1.000	1.000	1.000	1.000	1.000	1.000	1.000	1.000	1.000	1.000	1.000	1.000	1.000	1.000	1.000

Table 9: Best Accuracy for Different Models with Varying Sequence Length and Model Dimensions

a cosine annealing scheduler with 5% warmup ratio, the AdamW optimizer (learning rate = $1e-3$, weight decay = 0.01), and gradient clipping at 1.0.

Finetuning We employed a base learning rate of $1e-5$ for fine-tuning on the three individual datasets, with other training configurations remaining similar to those used in pre-training, except that RESONA modules benefited from a higher learning rate. For CoQA, NarrativeQA, and TriviaQA, we trained for 2k, 8k, and 10k steps, respectively. During general supervised fine-tuning, we created a unified training set by shuffling 10k samples from each of the three QA datasets, ensuring significant diversity in sequence length and content. Additionally, we constructed a general test set by selecting 500 validation samples from each dataset. We trained on this combined dataset for 4k steps.

C.5 NIAH Scoring Details

For the NIAH (Needle In A Haystack) task, we employ an automated scoring protocol based on prefix matching. The scoring methodology operates as follows: A full score of 5 points is awarded if the model’s response contains the complete and accurate needle. If not, we iteratively truncate the needle from the end (removing the last few characters incrementally) and perform prefix matching. Partial credit (a proportional fraction of the 5-point maximum) is granted when a truncated prefix matches exactly, with the remaining character percentage determining the awarded score. Responses containing no matching prefix of the needle receive 0 points. The final task score is obtained by averaging the scores across 100 test samples.